phys. stat. sol. (a) 62, 431 (1980)

Subject classification: 1.1 and 10.2

Institute of Solid State Physics, Academy of Sciences of the USSR, Chernogolovka[1]) *(a) and I. V. Kurchatov Institute of Atomic Energy, Moscow*[2]) *(b)*

Role of Entrance Slit in the X-Ray Section Topography of Single Crystals

By

V. V. Aristov (a), V. G. Kohn (b), and V. I. Polovinkina (a)

An investigation is made of the effect of the spectral-line width as well as of the dimension and position of the entrance slit on the diffraction image of a perfect crystal in the Lang experiment and in an experimental scheme with polychromatic focusing. Experimental results are given of the observation of the geometric image of the narrow slit as well as the changes of the fine structure of the diffraction pattern while changing the slit width and deviating the crystal from the exact Bragg condition. A theoretical analysis of the results observed is given in the approximation of geometric optics.

Представлены результаты исследования влияния ширины спектральной линии излучения, размера и положения входной щели на дифракционное изображение совершенного кристалла в экспериментальной схеме Ланга и в схеме с полихроматической фокусировкой. Приведены экспериментальные результаты наблюдения геометрического изображения узкой щели, изменений тонкой структуры дифракционной картины при изменении ширины щели и отклонении кристалла от точного условия Брэгга. Дан теоретический анализ наблюдаемых результатов в приближении геометрической оптики.

1. Introduction

Methods of the X-ray topography are finding a wide use for the study of the defect structure of crystals as well as for the quantitative analysis of elastic distortion fields in the vicinity of isolated defects [1 to 4]. In this case the necessity arises of a higher resolution of details of the contrast. This is accomplished in the experiment by decreasing the effective dimensions of the X-ray source focus and by eliminating the chromatic aberrations. Just for this purpose in section topography a narrow slit with a width of 10 to 20 μm is placed [5] in front of the crystal.

To interpret the section topographs the approximation of infinitely narrow slit has been usually employed in which the slit itself is regarded as a point source of spherical waves situated on the entrance surface of the crystal. At the same time the real slit width as well as the distances between the X-ray tube focus and the crystal (L_1) and also between the crystal and the film (L_2) are not taken into account at all.

The image of a perfect crystal under the condition of polychromatic focusing for symmetrical Laue-case diffraction and for $L_1 = L_2$ was investigated in details in [6 to 9]. These papers reveal a number of new interference effects, in particular, the focusing of the slightly absorbing mode of the X-ray wave field predicted theoretically in [10].

Naturally there arises the question of the effect of the entrance slit in front of the crystal on the real section topograph at different distances L_1 and L_2. It is this question in the most general formulation that the present paper is devoted to.

[1]) Chernogolovka 142432, Moscow district, USSR.

[2]) Moscow 123182, USSR.

2. Approximation of Geometrical Optics

The interference phenomena in the diffraction of a monochromatic spherical X-ray wave may be divided into several types depending on the distance $L = L_1 + L_2$ as shown in [9]. At the crystal thickness $t \approx t_s$ a focusing of the slightly absorbing mode of wave field occurs. The thickness of focusing is $t_s = K_s L$ where

$$K_s = 2 \cos\theta_B \frac{|\chi_{rh}| C_s}{\sin^2 2\theta_B}. \tag{2.1}$$

Here θ_B is the Bragg angle, χ_{rh} the Fourier component of the real part of the crystal polarizability $\chi = \chi_r + i\chi_i$, C_s the polarization factor. At $t \ll t_s$ and $t \gg t_s$ oscillations connected with the interference of the two modes of wave field are observed. In the case of $t \gg t_s$ the normal pendellösung effect (described by the Kato theory) occurs and in the case $t \ll t_s$ the anomalous one takes place.

As well as in [9] we consider symmetrical Laue diffraction but in addition we shall assume that a slit of width a is placed in front of the crystal in the X-ray path and the source radiates a packet of monochromatic waves with frequencies $\omega = \omega_0 + \Delta\omega$ where ω_0 corresponds to the maximum intensity in the spectrum, $\Delta\omega$ is of the order of the intrinsic halfwidth of the spectral line, Γ.

We shall carry out the analysis in the approximation of geometrical optics. Thereby naturally slit diffraction is not taken into account since the slit width in an X-ray experiment is much larger than the radiation wavelength. Consider a diffracted beam and introduce the base path that corresponds to the ray falling on the crystal at the Bragg angle for the frequency ω_0 (see Fig. 1). All other paths will be described using the parameter L and the coordinate x in the direction perpendicular to the base path: in front of the crystal along the vector $\boldsymbol{e}_{0\pi}$, within the crystal along the diffraction vector $\boldsymbol{h}$, and behind the crystal along the vector $\boldsymbol{e}_{h\pi}$. Here and below we use the same notations as in [9].

As shown in [9] each value of the angular deviation parameter y corresponds to a ray $x(L)$. The intensity at the point x is

$$I_h(x, \omega) = \frac{1}{2L^2} \sum_s \left| \sum_j z_j \frac{\exp\left(i\varphi_{sj}(y) - \mu_{sj}(y)\, t/2\right)}{2\sqrt{1+y^2}\sqrt{1 - \dfrac{z_j t}{t_s(1+y^2)^{3/2}}}} \right|^2. \tag{2.2}$$

Here the interference absorption coefficient μ_{sj} is determined in the conventional way, the parameter $z_j = 1$ for the slightly absorbing mode (B-type, $j = 1$) and $z_j = -1$ for the strongly absorbing mode (A-type, $j = 2$), the phase φ_{sj} is equal to

$$\varphi_{sj} = 2\pi \frac{K_s \sin^2\theta_B}{\lambda} \left(py + z_j t \sqrt{1+y^2} - \frac{1}{2} t_s y^2 \right). \tag{2.3}$$

In the case under consideration $p = (x - x_\omega)/t \sin\theta_B$ where x_ω determines the deviation of the path of the ray falling on the crystal at the Bragg angle for the frequency

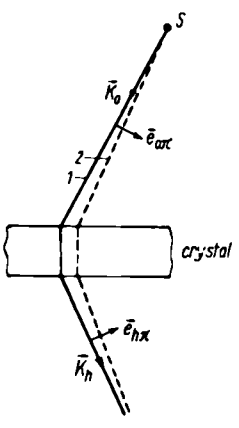

Fig. 1. Ray path scheme. 1 base path; $\boldsymbol{K}_h = \boldsymbol{K}_0 + \boldsymbol{h}$; 2 path of a ray entering the crystal at the Bragg angle for the frequency $\omega > \omega_0$

$\omega = \omega_0 + \Delta\omega$. The ray path $x(L)$ is described by the equation $\partial\varphi/\partial y = 0$ [9] which connects the angular variable y with the coordinate x at a fixed L,

$$x = x_\omega + \sin\theta_B\left(K_s L y - z_f t\,\frac{y}{\sqrt{1+y^2}}\right). \tag{2.4}$$

It is evident that in front of the crystal $x_\omega = \theta_\omega L\,(L \leq L_1)$, where $\theta_\omega = \operatorname{tg}\theta_B(\Delta\omega/\omega_0)$ and behind the crystal $x_\omega = \theta_\omega(L_1 - L_2)$. In the crystal itself $\sin\theta_B$ in equation (2.4) should be substituted by $\operatorname{tg}\theta_B$ (see Fig. 1),

$$x_\omega = x_{\omega c} = \frac{\theta_\omega L_1}{\cos\theta_B}.$$

In the simplest case a spectral line has the Lorentz form. Thereby the real pattern averaged over the spectrum is described by the expression

$$\overline{I_h(x)} = \frac{\gamma}{\pi}\int_{-\infty}^{\infty}\frac{d\theta_\omega}{(\theta_\omega^2 - \gamma^2)}\,I_h(x,\omega)\,, \tag{2.5}$$

where $2\gamma = \Gamma\operatorname{tg}\theta_B/\omega_0$ determines the halfwidth of a spectral line in terms of θ_ω.

If a slit in front of the crystal has sufficiently large dimension or is absent at all, the value $I_h(x,\omega)$ according to (2.3) and (2.4) depends on x and ω only in the form $(x - x_\omega)$. Therefore, in the case $L_1 \neq L_2$ non-monochromaticity leads to a diffusion of the interference pattern over a segment of the order of $2\gamma(L_1 - L_2)$ across the diffraction fringe.

To obtain a linear resolution on the topograph, e.g. of the order of 5 μm in the case $\operatorname{tg}\theta_B = 1/4$, $\Gamma/\omega_0 \approx 4 \times 10^{-4}$ is necessary for the condition $(L_1 - L_2) < 5$ cm to be satisfied.

3. Geometric Image of a Slit in Polychromatic Radiation

If a sufficiently narrow slit is placed in front of the crystal in the X-ray path the region of spectral diffusion will be determined by the slit dimension, the resulting diffraction pattern being not merely averaged but considerably distorted. Consider a point x_0 on the entrance surface of the crystal and determine the value of the angular deviation of the rays entering the crystal through this point. For each value of the frequency, i.e. $x_{\omega c}$, there exists a value of y determined from (2.4) in which $\sin\theta_B$ should be substituted by $\operatorname{tg}\theta_B$ and it should be set $t = 0$, $L = L_1$,

$$y = \frac{x_0 - x_{\omega c}}{K_s L_1 \operatorname{tg}\theta_B}. \tag{3.1}$$

The further ray path within the crystal is determined by the formulae

$$x = x_0 - z_f t\operatorname{tg}\varepsilon\,, \qquad \operatorname{tg}\varepsilon = \operatorname{tg}\theta_B\frac{y}{\sqrt{1+y^2}}. \tag{3.2}$$

If a spectral line is sufficiently broad, the angular variable y adopts all values up to $|y| \gg 1$. Thereby the rays corresponding to different frequencies form a "fan" with the vertex at the point x_0 and the angle $2\theta_B$. In this case the spectrum intensity inside the fan is distributed inhomogeneously. If the slit width is

$$a \ll 2\gamma L_1 \tag{3.3}$$

and the slit is on the base path for all the points inside the slit, the long "tails" of a spectral line satisfying the condition $|y| > 1$ fall on the fan edges, i.e. correspond to

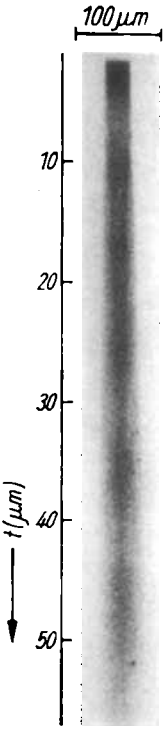

Fig. 2. Fragment of experimental section topograph illustrating a geometric image of the slit. Wedge-shaped Si specimen, AuL_α ($\lambda = 1.276$ Å) radiation, (220) reflection, $L_1 = 0.8$ m, $L_2 = 0.03$ m, $a = 25$ μm

scattering angles close to zero and $2\theta_B$. The main part of the incident polychromatic radiation intensity is propagated within the crystal just along these directions.

On the topograph placed behind the crystal when $L_2 \ll L_1$ this incoherent radiationforms two diffusion fringes the width of which is close to the slit dimension. If $a > 2t \operatorname{tg} \theta_B$ the fringes overlap, forming on the topograph an area of enhanced intensity which we call "a geometric image of the slit". The dimension of the image is equal to

$$a' = a - 2t \operatorname{tg} \theta_B . \tag{3.4}$$

The effect described has been observed experimentally on the topographs of wedge-shaped Ge and S icrystals for a number of symmetrical Laue reflections. As an example Fig. 2 shows the topograph of the thin part of a Si wedge for the (220) reflectio n.[3]) The width of the entrance slit is $a = 25$ μm, $L_1 = 0.8$ m, $L_2 = 0.03$ m. The value $2\gamma L_1 \approx 200$ μm [11] corresponds to these experimental conditions, therefore, inequality (3.3) is satisfied. The geometrical image of the slit in the topograph displays a triangle of enhanced intensity with the vertex directed towards the range of the greater thickness of the crystal. The altitude of the triangle when changing the slit width is changed according to (3.4). Besides, an enlargement of the entrance slit results in worsening the contrast of its geometric image. At the slit width $a \approx 2\gamma L_1$, the intensity distribution becomes integral, and the area of enhanced intensity is not observed.

When $L_2 = L_1$ the geometrical image of the slit is not observed because of the polychromatic focusing.

4. Asymmetry of the Fringes of the Anomalous Pendellösung Effect

If the crystal is located midway between the source and the detector ($L_1 = L_2$), the role of a slit (even of relatively large dimension) is primarily a limitation of the spectrum of frequencies for which the interference of the wave fields of A and B modes belonging to different branches of the dispersion surface is possible.

Fig. 3 shows two topographs of the thin part of a Ge wedge for reflection (111) obtained in the experimental scheme with $L_1 = L_2 = 1.15$ m. The slit width was identical in the two cases and was very large, $a = 2$ mm. In the case presented in Fig. 3a the slit was located near the base line and in the case of Fig. 3b at a considerable distance from it. The image of a perfect crystal in Fig. 3a is formed by the central part of the spectrum the effective halfwidth ($\tilde{\Gamma}/\omega_0$) of which is of the order of $a/2L_1 \operatorname{tg} \theta_B \approx 4 \times 10^{-3}$ that considerably exceeds the intrinsic line halfwidth $\Gamma/\omega_0 \approx 4 \times 10^{-4}$ [11]. Thus, the slit almost does not affect the pattern obtained.

[3]) All the topographs were obtained with the Microflex device Rigaku Denki using AuL_α radiation ($\lambda = 1.276$ Å).

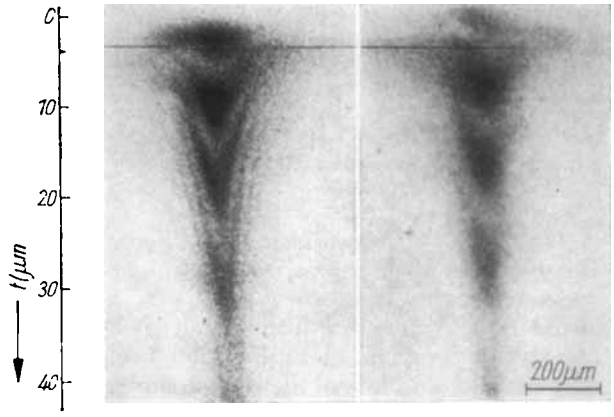

Fig. 3. Fragments of wedge-shaped Ge crystal topographs in the scheme with polychromatic focusing ($L_2 = L_1$). (111) reflection, AuL_α($\lambda = 1.276$ Å) radiation, $L = L_1 + L_2 = 2.3$ m, $a = 2.0$ mm. a) The crystal is in the Bragg position for the centre of a spectral line, $\theta - \theta_B = 0$. b) The crystal deviates from the exact Bragg condition for the central part of the spectrum, $\theta - \theta_B \neq 0$

Quite another situation occurs in Fig. 3b. Here the Bragg condition is satisfied exactly only for the spectral line "tail". Whereas the central part of the spectrum penetrates into the crystal at incidence angles corresponding to the deviation from the Bragg condition described by the parameter y of only one sign. In accordance with (2.4) the interference pattern is observed only on one side from the base line (the coordinate x being of constant sign) if $t \ll K_3 L$. Considerable worsening of the contrast is connected with the presence of a large interval of frequencies where interference is impossible at all, since for all slit points A-mode rays are not scattered, whereas B-mode rays are scattered at an angle $2\theta_B$ (or vice versa in the case of the opposite direction of the slit displacement). Thereby the B-mode rays (focusing) form a background in the area of the interference pattern.

A reduction of the slit dimension results in the limitation of the interval of frequencies being subject to diffraction reflection and, consequently, in diminishing the intensity of the reflected beam. The diffraction pattern itself changes as well in this case, especially in the area corresponding to the thin part of the wedge. As the slit width decreases the diffraction image in this area is narrowed in such a way that its dimensions exceed those of the slit. The latter is due to a polychromatic focusing phenomenon in consequence of which all the frequencies contribute to the image at the same place of the film. Thereby the off-Bragg frequencies lead to the formation of asymmetric diffraction patterns being peripheral fragments of the general pattern arising in the absence of a slit. These fragments are composed with the central ones to form a mosaic structure which results in an effective broadening of the diffraction fringe.

However, to observe such a reconstructed diffraction pattern in the case of a narrow slit it is necessary to have either a very strong source or very long exposures. When the exposure is short the film fixes only a part of the diffraction pattern corresponding to the maximum intensity. Fig. 4a shows the topograph of the thin part of a Ge wedge in the case of (220) reflection, $L_2 = L_1 = 85$ cm. The slit was located on the base path and had a size $a = 0.3$ mm. The maximum width of the diffracted fringe observed was about 0.15 mm which is due to insufficient exposure as far as the latter was chosen from the requirement that the optimum contrast of the interference pattern should be attained.

Besides in the case of asymmetric position of the slit (off the base path) we have observed a specific curvature of the diffraction fringe. Fig. 4b shows the photograph obtained under the same condition as Fig. 4a, but for another position of the slit. In this figure it is clearly seen that the diffraction fringe strongly bends and slightly

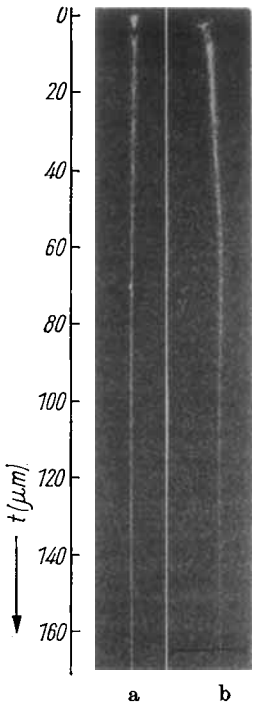

Fig. 4. Topographs of a wedge-shaped Ge crystal obtained in the scheme $L_2 = L_1$ (reversed contrast). (220) reflection, AuL_α ($\lambda = 1.276$ Å) radiation, $L = L_1 + L_2 = 1.7$ m. a) Slit width $a = 300$ μm, exact Bragg position for the centre of a spectral line, $\Delta\theta_B = 0$. b) $a = 300$ μm, the crystal deviates from the exact diffraction condition for the central part of the spectrum, $\Delta\theta_B \neq 0$. (The length indicated corresponds to 1000 μm)

widens in the region corresponding to the thin part of the wedge, the deviation of the fringe from a straight line considerably exceeding the slit dimension.

The nature of a diffraction fringe bend is of interest. When the exposure is short, the diffraction fringe in the thin part of the wedge is formed by the frequency interval corresponding to the intensity maximum in the AuL_α line spectrum. The radiation in this frequency interval is incident on the crystal at an angle that considerably differs from the Bragg one. Therefore, the observed fringe is a peripheral fragment of the general diffraction pattern which would be considerably wider in the absence of a slit. As the crystal thickness increases, a focusing of the reflected X-ray occurs (see (2.2)). The intensity maximum in this area coincides with the frequency interval for wihch the slit is in the Bragg position. As a result the fringe is straightened.

5. The Effect of the Entrance Slit on the Normal Pendellösung Effect and Focussing

Consider the area of the diffraction pattern corresponding to the condition $t \geqq t_s$. To do this let us analyse the A- and B-mode ray paths inside and outside the crystal and find the points x_{0A} and x_{0B} at which the rays of the A- and B-modes arriving of the same point of the film x penetrate into the crystal. To accomplish this we use (2.4) and (3.1) assuming $x_\omega = 0$ in (2.4). The thickness of focusing is $t_s = K_s L = 2K_s L_1$. It follows from (3.1) that

$$x_{0A,B} = x_{\omega c} + \tfrac{1}{2} t_s y_{A,B} \operatorname{tg} \theta_B , \tag{5.1}$$

where $y_{A,B}$ according to (2.4) are determined by

$$\frac{x}{t_s \sin\theta_B} = y_A + \frac{t}{t_s}\frac{y_A}{\sqrt{1+y_A^2}} = y_B - \frac{t}{t_s}\frac{y_B}{\sqrt{1+y_B^2}}. \tag{5.2}$$

Since $t \gg t_s$ the solutions of (5.2) for which $|y| \ll 1$ are of utmost importance. Neglecting $y^2_{A,B}$ as compared with unity we obtain

$$x_{0A} = x_{\omega c} + \frac{x'}{2}\frac{t_s}{t+t_s}, \qquad x_{0B} = x_{\omega c} - \frac{x'}{2}\frac{t_s}{t-t_s}. \tag{5.3}$$

Here and below $x' = x/\cos\theta_B$.

Thus, the points x_{0A} and x_{0B} are situated on different sides of the central point $x_{\omega c}$ corresponding to the Bragg direction for the frequency ω at a distance that is considerably less than $|x|$ in the case of $t \gg t_s$. In other words, the large central area of the diffraction pattern is formed by a relatively narrow section of the entrance surface of the crystal near $x_{\omega c}$. If the slit width a is sufficiently small, the dimension of the visible

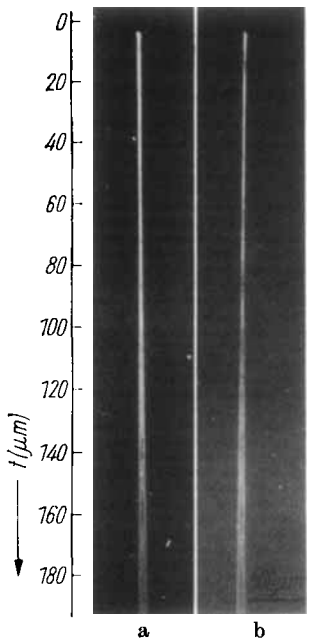

Fig. 5. Topographs of a wedge-shaped Si crystal obtained in the scheme with $L_2 = L_1$ (reversed contrast). (220) reflection, AuL_α ($\lambda = 1.276$ Å) radiation, $L = L_1 + L_2 = 0.8$ m. a) Entrance slit width $a = 300$ μm; b) $a = 25$ μm

diffraction pattern is determined by the formula

$$\Delta x \approx \frac{a}{K_s L_1} t . \tag{5.4}$$

On the other hand, the natural dimension of the diffraction pattern (without a slit) does not exceed $2t \sin \theta_B$. Consequently, if

$$y_0 = \frac{a}{2K_s L_1 \sin \theta_B} > 1 , \tag{5.5}$$

the slit does not spoil the diffraction pattern. The latter however is formed only by the frequencies for which the slit is in the Bragg position.

The conclusion we have drawn is confirmed by the experimental results. Fig. 5 presents two topographs of an ideal Si crystal in the case of (220) reflection and $L_1 = L_2 = 0.4$ m. The width of the entrance slit is equal to 300 μm (Fig. 5a) and 25 μm (Fig. 5b). In this case $t_s = 24$ μm, $\sin \theta_B = 0.332$, therefore (5.5) is satisfied. As seen from Fig. 5 the images are almost not different, but the topograph Fig. 5b is clearer than topograph Fig. 5a. One of possible reasons explaining this fact lies in that in the experiment the condition of symmetric Laue diffraction has not been fulfilled with sufficient accuracy. Thereby photograph Fig. 5a proved to be more diffuse, since it is formed by a larger frequency interval than photograph Fig. 5b.

The conclusion on the diffraction pattern stability with respect to diminishing slit dimension is equally valid for the phenomenon of focusing. The intensity is collected at the focus due to the convergence of rays within the angle interval $|y| < Y_s$, where [9]

$$Y_s = \frac{1}{2} \left(\frac{4}{\pi \sin \theta_B} \frac{\lambda L}{t_s^2} \right)^{1/4} . \tag{5.6}$$

Thereby the focusing X-ray beam has the width $\Delta x = Y_s t_s \sin \theta_B$ in the region in front of the crystal. If the slit width exceeds this value, the effect of focusing remained unchanged for the frequencies at which the slit "is seen" under the Bragg angle. As the slit dimension decreases the intensity at the focus decreases but the effect of focusing shows itself very clearly. The intensity ratio at the focus to the background even improves. This is clearly seen from Fig. 5a and b.

Now let be $L_2 \ll L_1$ (the film being situated immediately behind the crystal). In this case it is also easy to find the points x_{0A}, x_{0B} and then to determine the dimensions of the visible diffraction pattern. As a result we obtain condition (5.5) again. However, the experimental scheme with $L_2 \ll L_1$ has an essential, distinguishing feature in that different frequencies give diffraction patterns on the film shifted by $x_\omega = \theta_\omega L_1$. Thereby the role of the entrance slit, as a limiter of the frequency interval involved in the interference, abruptly increases since in the absence of the slit the diffraction

pattern would be diffused over a section with the length $2\gamma L_1$ (see (2.5)) which considerably exceeds the width of the diffraction pattern itself. In the case of the experiment with a slit the diffusion occurs only over a section with a width equal to that of the slit a. In the thickness range $t \gg K_s L_1$, according to (5.4) the dimension of the visible diffraction pattern $\Delta x \gg a$, therefore the contrast does not disappear completely.

Note that the width of a diffraction fringe for $t \gg K_s L_1$ does not exceed $2t \sin \theta_B$ and the pattern of pendellösung fringes proves to be edged by regions with a practically constant blackening. It is in these regions that the rays of either A- or B-mode (each separately) corresponding to the tails of a spectral line $|x_\omega| > a/2$ penetrate. Indeed in this case we have instead of (5.3)

$$x_{0A} = x_{\omega c} + (x' - x_{\omega c}) \frac{t_s}{(t + t_s)}, \qquad x_{0B} = x_{\omega c} - (x' - x_{\omega c}) \frac{t_s}{(t - t_s)}, \tag{5.7}$$

where $t_s = K_s L$. Provided the condition $|x_\omega| > a/2$ is fulfilled it follows from (5.7) that both the points x_{0A} and x_{0B} cannot be situated inside the slit at the same time in the case $t \gg t_s$. If the contrary is the case, such a possibility exists and leads to the formation of a geometric image of the slit we have considered in Section 2.

The width of the polychromatic fringes, generally speaking, increases with the growth of t and may exceed the slit width. We shall demonstrate this for the case when the slit is in the base path and $x_\omega = 0$. The interference requires (see (3.2))

$$\left.\begin{aligned} & x' = x_{0A} + t \operatorname{tg} \varepsilon_A = x_{0B} - t \operatorname{tg} \varepsilon_B , \\ & \operatorname{tg} \varepsilon_{A,B} = \operatorname{tg} \theta_B \frac{y_{A,B}}{\sqrt{1 + y_{A,B}^2}}, \qquad y_{A,B} = \frac{x_{0A,B}}{t_s \operatorname{tg} \theta_B}, \\ & |x_{0A}|, |x_{0B}| < \frac{a}{2 \cos \theta_B} . \end{aligned}\right\} \tag{5.8}$$

Conditions (5.8) are satisfied only in the triangular area with the vertex at the point $x' = 0$, $t = t_s$, and the angle $\varepsilon < \theta_B$, if $y_0 \leqq 1$. In the case of $y_0 \ll 1$ it is easy to see from (5.8) that $\operatorname{tg} \varepsilon = a/(2t_s \cos \theta_B)$. The scheme of domains in a crystal with interference contrast and without it is shown in Fig. 6.

Fig. 7 represents the complete topograph a fragment of which is shown in Fig. 2. It corresponds to the same experimental conditions as photograph Fig. 5b but with $L_1 = 0.8$ m, $L_2 = 0.03$ m. Comparing Fig. 5b and 7 it is easy to see that although $L = L_1 + L_2$ in both cases is almost identical and the slit has the same dimension. Fig. 7 differs from Fig. 5b due to frequency diffusion in some respects: firstly by a weaker contrast, secondly by a "background frame". In the given case $y_0 \approx 1.5$ therefore the width of polychromatic fringes is approximately equal to the slit width.

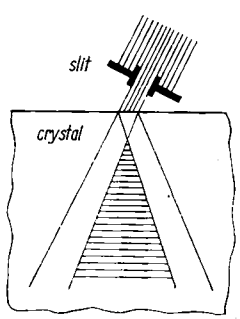

Fig. 6. Scheme of ray paths within the crystal. The region reached by the rays corresponding ot two branches of the dispersion surface (A- and B-modes) is shaded

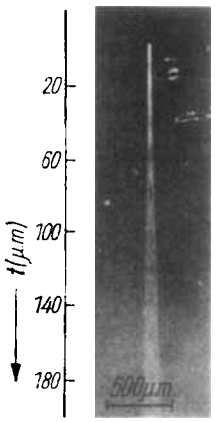

Fig. 7. The topograph of a wedge-shaped Si crystal obtained in the scheme with $L_2 \ll L_1$ and a narrow entrance slit. (220) reflection, $AuL_\alpha(\lambda = 1.276$ Å) radiation, $L_1 = 0.8$ m, $L_2 = 0.03$ m, $a = 25$ μm

Note that in Fig. 5 and 7 the range of thicknesses $t \approx 15$ to 35 μm corresponds to a focusing of the wave field (for $L = 0.8$ m $t_s = 24$ μm). This is associated with the fact that in Fig. 7 the diffraction fringe width in the above-mentioned thickness range is almost constant and approximately equal to the slit width ($\Delta x \approx a$), and only with further increase of the thickness it starts to increase in the regular way.

6. Conclusions

The results presented in the previous sections clearly show the role of the entrance slit in the formation of the diffracted image of a perfect crystal in two experimental schemes: Lang's conventional scheme ($L_2 \ll L_1$) and the scheme with polychromatic focusing ($L_2 = L_1$).

In both schemes the diminution of the slit dimension results in narrowing the wavelength interval for which the diffraction condition is satisfied. This fact is essential in Lang's section topography ($L_2 \ll L_1$). Here a narrow slit in front of the crystal is an obligatory part of the experimental scheme. Thereby the interference pattern is clearly observed in the crystal thickness range $t > t_s$. Pendellösung fringes are observed only partly at small thicknesses $t < t_s$. The geometric image of the slit is an important detail of the diffraction pattern.

In the case of $L_2 = L_1$ all types of interference pattern (focusing, pendellösung effect) are observed at almost any width of the slit except for the case of very small dimensions, when diffraction phenomena at the slit are of importance.

The possibility to observe a dynamic focusing of an X-ray wave field on a single crystal in the scheme with $L_2 \ll L_1$ is a result important for the practice. The focusing on one crystal block may prove sensitive to distortions of the crystal structure just as in the case of focusing in a bicrystal interferometer [12]. This provides new opportunities for the development of experimental methods applied in the investigation of elastic stress fields in crystals.

References

[1] N. Kato, Acta Cryst. **16**, 282 (1963).
[2] E. V. Suvorov, O. S. Gorelik, V. M. Kaganer, and V. L. Indenbom, phys. stat. sol. (a) **54**, 29 (1979).
[3] J. R. Patel and N. Kato, J. appl. Phys. **44**, 971 (1973).
[4] R. N. Kütt, P. V. Petrashen, I. L. Shulpina, and A. S. Tregubova, Proc. IV. Conf. Dynamic Effects of X-Ray and Electron Scattering, LIYaF, Leningrad, 1977 (p. 168) (in Russian).
[5] A. R. Lang, J. appl. Phys. **29**, 567 (1958).
[6] V. V. Aristov, V. I. Polovinkina, I. M. Shmytko, and E. V. Shulakov, Zh. eksper. teor. Fiz., Pisma **28**, 6 (1978).
[7] V. D. Kozmik and I. P. Mikhailyuk, Ukr. fiz. Zh. **23**, 1570 (1978); Zh. eksper. teor. Fiz., Pisma **28**, 673 (1978).

[8] V. V. ARISTOV and V. I. POLOVINKINA, Acta Cryst. **A34**, 227 (1978).
[9] V. V. ARISTOV, V. I. POLOVINKINA, A. M. AFANASEV, and V. G. KOHN, Acta Cryst., in the press.
[10] A. M. AFANASEV and V. G. KOHN, Fiz. tverd. Tela **19**, 1775 (1977).
[11] I. H. WILLIAMS, Phys. Rev. **45**, 71 (1934).
[12] E. V. SUVOROV, V. I. NIKITENKO, and K. YU. MUKHIN, phys. stat. sol. (a) **50**, 213 (1978).

(Received July 14, 1980)